



PERGAMON

Computers in Biology and Medicine 31 (2001) 399–406

---

---

Computers in Biology  
and Medicine

---

---

www.elsevier.com/locate/complbiomed

# The use of the Hilbert transform in ECG signal analysis

D. Benitez<sup>a</sup>, P.A. Gaydecki<sup>a,\*</sup>, A. Zaidi<sup>b</sup>, A.P. Fitzpatrick<sup>b</sup>

<sup>a</sup>*Department of Instrumentation and Analytical Science, University of Manchester Institute of Science and Technology (UMIST), P.O. Box 88, Manchester M60 1QD, UK*

<sup>b</sup>*Manchester Heart Centre, The Royal Infirmary, Oxford Road, Manchester M13 9WL, UK*

Received 16 June 2000; accepted 16 January 2001

---

## Abstract

This paper presents a new robust algorithm for QRS detection using the first differential of the ECG signal and its Hilbert transformed data to locate the *R* wave peaks in the ECG waveform. Using this method, the differentiation of *R* waves from large, peaked *T* and *P* waves is achieved with a high degree of accuracy. In addition, problems with baseline drift, motion artifacts and muscular noise are minimised. The performance of the algorithm was tested using standard ECG waveform records from the MIT-BITH Arrhythmia database. An average detection rate of 99.87%, a sensitivity (Se) of 99.94% and a positive prediction (+*P*) of 99.93% have been achieved against study records from the MIT-BITH Arrhythmia database. A detection error rate of less than 0.8% was achieved in every study case. The reliability of the proposed detector compares very favorably with published results for other QRS detectors. © 2001 Elsevier Science Ltd. All rights reserved.

*Keywords:* ECG signal detection; Hilbert transform; Artifacts; Electrocardiography

---

## 1. Introduction

Accurate determination of the QRS complex, in particular, accurate detection of the *R* wave peak, is essential in computer-based ECG analysis. However, this is often difficult to achieve. Noise contamination, due to baseline drifts changes, motion artifacts and muscular noise, is frequently encountered [1]. In addition, morphological differences in the ECG waveform increase the complexity of QRS detection, due to the high degree of heterogeneity in the QRS waveform and the difficulty in differentiating the QRS complex from tall peaked *P* or *T* waves [2].

Many different approaches have been used to improve the accuracy of QRS detection, including the use of the Hilbert transform. The use of the Hilbert transform in ECG analysis was first described by Bolton and Westphal [3–6]. In general, this method of ECG waveform analysis uses

---

\* Corresponding author. Tel.: +44-161-200-4906; fax: +44-161-200-4911.

*E-mail address:* p.a.gaydecki@umist.ac.uk (P.A. Gaydecki).

vectorcardiograph and polarcardiograph representations and examines the concept of pre-envelope and envelope of a real waveform given by the Hilbert transform. They developed a prototype two stage QRS detector based on the determination of a zero crossing in the Hilbert transformed data of the original ECG waveform coincident with a large magnitude in its envelope.

In this paper, a new approach to QRS detection using other properties of the Hilbert transform is presented. The new algorithm uses the first differential of the ECG signal and its Hilbert transformed data to find regions of high probability to locate the *R* peaks in the ECG waveform. Similar to the method developed by Bolton and Westphal, a second stage detection algorithm uses these initial estimations to locate the real *R* peaks in the ECG wave. This has a number of advantages over previously described techniques. The unwanted effects of large peaked *T* and *P* waves are minimized and the new algorithm performs excellently in the presence of significant noise contamination. Moreover, in contrast to the method of Bolton and Westphal, determination of the envelope and pre-envelope of the given data is not required.

## 2. The Hilbert transform

Given a real time function  $x(t)$ , its Hilbert transform [7,8] is defined as

$$\hat{x}(t) = H[x(t)] = \frac{1}{\pi} \int_{-\infty}^{\infty} x(\tau) \frac{1}{t - \tau} d\tau. \quad (1)$$

It can be seen from (1) that the independent variable is not changed as result of this transformation, so the output  $\hat{x}(t)$  is also a time dependent function. Furthermore,  $\hat{x}(t)$  is a linear function of  $x(t)$ . It is obtained from  $x(t)$  applying convolution with  $(\pi t)^{-1}$  as shown in the following relationship:

$$\hat{x}(t) = \frac{1}{\pi t} * x(t) \quad (2)$$

rewriting (2) and applying the Fourier transform, we have

$$F\{\hat{x}(t)\} = \frac{1}{\pi} F\left\{\frac{1}{t}\right\} F\{x(t)\}. \quad (3)$$

Since,

$$F\left\{\frac{1}{t}\right\} = \int_{-\infty}^{\infty} \frac{1}{x} e^{-j2\pi f x} dx = -j\pi \operatorname{sgn} f, \quad (4)$$

where

$$\operatorname{sgn} f \text{ is } +1 \text{ for } f > 0, \text{ } 0 \text{ for } f = 0 \text{ and } -1 \text{ for } f < 0$$

then the Fourier transform of the Hilbert transform of  $x(t)$  is given by (3) as

$$F\{\hat{x}\} = -j \operatorname{sgn} f F\{x(t)\}. \quad (5)$$

In the frequency domain, the result is then obtained by multiplying the spectrum of the  $x(t)$  by  $j (+90^\circ)$  for negative frequencies and  $-j (-90^\circ)$  for positive frequencies. The time domain result can be obtained performing an inverse Fourier transform. Therefore, the Hilbert transform of the original function  $x(t)$  represents its harmonic conjugate [8].

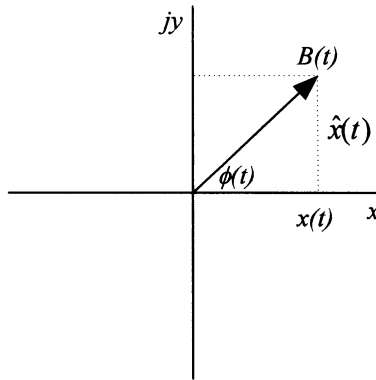


Fig. 1. Complex representation of the envelope.

In considering the concept of analytic signal or pre-envelope of a real signal  $x(t)$  [9], it can be described by the expression:

$$y(t) = x(t) + j\hat{x}(t). \quad (6)$$

The envelope  $B(t)$  of  $y(t)$  is defined by

$$B(t) = \sqrt{x^2(t) + \hat{x}^2(t)} \quad (7)$$

and its instantaneous phase angle in the complex plane can be defined by

$$\phi(t) = \arctan\left(\frac{\hat{x}(t)}{x(t)}\right). \quad (8)$$

As shown in the Fig. 1  $B(t)$  and  $x(t)$  have common tangents and the same values at the points where  $\hat{x}(t) = 0$ , i.e., the envelope determined using (7) will have the same slope and magnitude of the original signal  $x(t)$  at or near its local maxima. Similarly, from (7) it can be seen that  $B(t)$  is always a positive function. Hence, the maximum contribution to  $B(t)$  at points where  $x(t) = 0$  is given by the Hilbert transform. This can be easily seen in Fig. 2 where the maximum contribution to the envelope of the first differential of the ECG  $B(d/dt(\text{ECG}))$  is given by its Hilbert transform  $H[d/dt(\text{ECG})]$  at points where  $d/dt(\text{ECG}) = 0$ .

### 3. The new approach to QRS detection using the Hilbert transform

One of the properties of the Hilbert transform is that it is an odd function. That is to say that it will cross zero on the  $x$ -axis every time that there is an inflexion point in the original waveform (Fig. 2). Similarly a crossing of the zero between consecutive positive and negative inflexion points in the original waveform will be represented as a peak in its Hilbert transformed conjugate. This interesting property can be used to develop an elegant and much easier way to find the peak of the QRS complex in the ECG waveform corresponding to a zero crossing in its first differential waveform  $d/dt(\text{ECG})$ . The block diagram of the proposed approach is shown in Fig. 3.



Fig. 2. ECG Contributions to the envelope  $B[d/dt(ECG)]$ , where  $d/dt(ECG)$  is the first differential of the ECG waveform and  $H(d/dt(ECG))$  is its Hilbert transform.

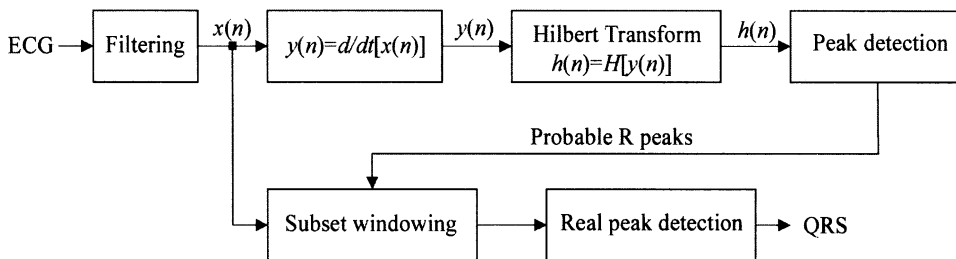


Fig. 3. Block diagram of the QRS detector.

As with most QRS detector algorithms, the first stage of the proposed algorithm is formed by a filtering section [10]. We used a band pass FIR filter windowed using a Kaiser–Bessel window. The band stop frequencies were set at 8 and 20 Hz in order to remove muscular noise and maximize the QRS complex respectively. Then, the first differential of the resulting filtered sequence is performed in order to remove motion artifacts and base line drifts. The rising slope of the *R* wave will be represented as a maximum and the falling slope will be represented as a minimum in the first

differential sequence. The peak of the  $R$  wave will be equivalent to the zero crossing between these two positive and negative peaks (see Fig. 2).

So given the filtered ECG waveform sequence  $x(n)$ , its first differential ( $y(t) = d/dt(\text{ECG})$ ) in discrete domain can be obtained by

$$y(n) = \frac{1}{2\Delta t}[x(n+1) - x(n-1)] \quad \text{for } n = 0, 1, 2, \dots, m-1, \quad (9)$$

where  $m$  is the total number of samples and  $\Delta t$  is the sampling frequency.

The initial condition is specified by  $x(-1)$  when  $n=0$ , and the final condition  $x(m)$  when  $n=m-1$ . These conditions minimize the error at the boundaries. The Hilbert transform  $h(n)$  of the sequence  $y(n)$  that represents the first differential of the ECG waveform is then obtained using the following methodology:

1. Obtain the Fourier transform  $F(n)$  of the input sequence  $y(n)$ ,
2. set the DC component to zero,
3. multiply the positive and negative harmonics by  $-j$  and  $j$  respectively,
4. perform the inverse Fourier transform of this resulting sequence.

Since this algorithm for Hilbert transformation works well with short sequences, a moving 1024 points window is used to subdivide the input sequence  $y(n)$  before obtaining its Hilbert transform. In this work, the sample frequency used was 360 Hz. To optimize accuracy, the starting point of the next window should match the last  $R$  point located in the previous ECG subset.

The peaks in the Hilbert transformed sequence  $h(n)$  represent regions of high probability of finding a real QRS peak. In practice, these peaks often differ from the true  $R$  wave peak position by a few milliseconds. In order to guarantee accurate detection of the  $R$  peaks, a second stage detector is required. Because the  $P$  and  $T$  waves are minimized in relation to the relative peak corresponding to QRS complex in the Hilbert sequence, a simple threshold detection is used to locate the peaks in the  $h(n)$  sequence. The threshold must be adaptive in order to guarantee accurate detection of the  $R$  peaks. The threshold level is set using the following criteria: first the level of noise present in the subset under analysis is determined using the equivalent RMS value of the  $h(n)$  sequence and its maximum amplitude in the window, if the RMS value is equal or greater than 18% of the maximum value of the  $h(n)$  sequence, the level of noise in the segment is considered to be high and therefore the threshold level is setup at 39% of the maximum amplitude of  $h(n)$ , if the maximum value of the sequence under study is greater than two times the amplitude of the maximum value of the previous subset window of 1024 points, then the threshold is raised to 39% of the maximum amplitude of the previous subset  $h(n)$ . When the RMS value is lower than 18% of the maximum value of the  $h(n)$  sequence, the amount of noise in the subset is considered to be low and the threshold level is decreased to 1.6 times the RMS value. If two peaks in the Hilbert sequence  $h(n)$  are located very close each other (less than 200 ms), only one of the peak has probabilities of a real  $R$  peak. The decision is made in base of the amplitude of the peak and their position in relation to the last  $R$  peak located using an adaptive time threshold based on the average  $R$ – $R$  interval length of the previous  $R$  peaks located.

The second stage detector uses the information provided by the first approximation. A defined width window subset (i.e.,  $\pm 10$  samples form the location of the peak found in the corresponding

Table 1  
QRS detection performance using the MIT-BIH database

MIT-BIH record	Actual number of beats in record	FP	FN	Failed detection (FP+FN)	Detection error rate (%)	Average timer error (ms)	Se (%)	+P (%)
100	2273	0	0	0	0.00	0.40	100	100
101	1865	3	1	4	0.21	0.32	99.95	99.84
102	2187	1	2	3	0.14	2.58	99.91	99.95
103	2084	0	0	0	0.00	0.14	100	100
104	2229	12	5	17	0.76	2.84	99.78	99.46
105	2572	7	3	10	0.39	0.63	99.88	99.73
106	2027	1	0	1	0.05	1.34	100	99.95
107	2137	1	7	8	0.37	1.75	99.67	99.95
109	2532	1	7	8	0.32	0.96	99.72	99.96
111	2124	1	1	2	0.09	0.99	99.95	99.95
112	2539	0	0	0	0.00	0.34	100	100
113	1795	0	0	0	0.00	0.13	100	100
114	1879	1	0	1	0.05	1.03	100	99.95
115	1953	0	0	0	0.00	0.29	100	100
116	2412	0	0	0	0.00	41.40	100	100
117	1535	1	1	2	0.13	8.45	99.93	99.93
118	2278	1	0	1	0.04	0.28	100	99.96
119	1987	1	0	1	0.05	0.63	100	99.95
121	1863	0	1	1	0.05	0.44	99.95	100
122	2476	0	0	0	0.00	0.27	100	100
123	1518	1	0	1	0.07	0.12	100	99.93
124	1619	0	0	0	0.00	1.31	100	100
Average	45856	30	28	58	0.13	3.03	99.94	99.93

$h(n)$  sequence) is selected in the original ECG waveform to locate the real  $R$  peak. Once again a simple maximum peak locator in the values of this subset sequence is used.

#### 4. Results and discussion

The detector was tested using entire records from the MIT-BIH Arrhythmia database [11]. From this database a set of ECG waveform signals recorded using the modified limb lead II (MLII) and modified leads V5 and V1 ECG electrodes configuration which contain mechanical and electrical artifacts was chosen to test the performance of the new algorithm. Beat by beat comparison was performed according to the recommendation of the American National Standard for ambulatory ECG analyzers (ANSI/AAMI EC38-1994) [12]. The results are shown in Table 1. A false negative (FN) occurs when the algorithm fails to detect a true beat (actual QRS) quoted in the corresponding annotation file of the MIT-BIH record and a false positive (FP) represents a false beat detection. Sensitivity (Se) [12], positive prediction (+P) [12], detection error rate [13] and average time error were calculated using the following equations respectively:

$$\text{Sensitivity (\%)} = \frac{\text{TP}}{\text{TP} + \text{FN}} \%, \quad (10)$$

Table 2

Performance comparison with other detectors For noisy MIT-BIH record 105 containing 2572 QRS complex

Method	FP	FN	Failed detection	Detection error rate (%)	Se (%)	+P (%)	Reference
Proposed detector	7	3	10	0.39	99.88	99.73	
Neural-based adaptive filtering	10	4	14	0.54	99.84	99.61	[13]
Wavelet transforms	15	13	28	1.09	99.50	99.42	[14]
Topological mapping	41	4	45	1.75	99.84	98.43	[15]
Optimized filtering and dual edge thresholding	35	21	56	2.18	99.19	98.66	[16]
Linear adaptive filtering	40	22	62	2.41	99.15	98.47	[13]
Bandpass filtering and search-back	53	22	75	2.91	99.15	97.98	[10]
Bandpass filtering	67	22	89	3.46	99.15	97.46	[17]
Filter banks <sup>a</sup>	53	16	69	3.22	99.26	97.58	[18]

<sup>a</sup>This result reported over 2139 beats only.

$$\text{Positive predictivity (\%)} = \frac{\text{TP}}{\text{TP} + \text{FP}}\%, \quad (11)$$

$$\text{Detection error rate (\%)} = \frac{\text{FP} + \text{FN}}{\text{Total number of QRS complex}}\%, \quad (12)$$

$$\text{Average time error (ms)} = \frac{\sum_{i=0}^{\text{TP}} |\text{located QRS} - \text{actual QRS}|}{\text{TP}}, \quad (13)$$

where TP (true positives) is the total number of QRS correctly located by the detector. The detector shows outstanding performance for signal with noise even in the presence of pronounced muscular noise and baseline artifacts. The reliability of the proposed detector compares very favorably with published results for other QRS detectors especially for the difficult noisy MIT-BIH record 105. The predominant features of this record are high grade of noise and artifacts [11]. Comparative results are shown in the Table 2.

## 5. Conclusion

This paper presents a new approach to QRS detection using properties of the Hilbert transform. Using the MIT-BIH arrhythmia database, the algorithm performed highly effectively with accurate QRS peak detection in over 99% of cases, even in the presence of significant noise contamination. At present, the algorithm performs significantly better with the MLII configuration than with other ECG leads. However, we believe that with further modification, this approach will provide the most accurate method of QRS detection for all ECG configurations.

## References

- [1] G.M. Friesen, T.C. Jannett, M.A. Jadallah, S.L. Yates, S.R. Quint, H.T. Nagle, A comparison of the noise sensitivity of nine QRS detection algorithms, *IEEE Trans. Biomed. Eng.* 37 (1990) 85–98.
- [2] N.V. Thakor, J.G. Webster, W.J. Thompkins, Estimation of QRS complex power spectra for design of a QRS filter, *IEEE Trans. Biomed. Eng.* 31 (1984) 702–705.

- [3] R.J. Bolton, L.C. Westphal, Hilbert transform processing of ECG's, 1981 IREECON International Convention Digest, IREE, Melbourne, 1981, pp. 281–283.
- [4] R.J. Bolton, L.C. Westphal, Preliminary results in display and abnormality recognition of Hilbert Transformed e.c.g.s, Med. Bio. Eng. Comput. 19 (1981) 377–384.
- [5] R.J. Bolton, L.C. Westphal, On the use of the Hilbert Transform for ECG waveform processing, in: Computers in Cardiology, IEEE Computer Society, Silver Spring, MD, 1984, pp. 533–536.
- [6] R.J. Bolton, L.C. Westphal, ECG display and QRS detection using the Hilbert Transform, in: K.L. Ripley (Ed.), Computers in Cardiology, IEEE Computer Society, Washington, DC, 1985, pp. 463–466.
- [7] R.N. Bracewell, The Fourier Transform and its Applications, McGraw-Hill, New York, 1978, pp. 267–274.
- [8] Analogic, Universal waveform analyzer, Application Note No. 301 (Advanced Math), Analogic Ltd., pp. I301-1–I301-5.
- [9] A.V. Oppenheim, R.W. Schaffer, Discrete-Time Signal Processing, Prentice-Hall, Englewood Cliffs, NJ, 1989, p. 775.
- [10] P.S. Hamilton, W.J. Tompkins, Quantitative investigation of QRS detection rules using the MIT/BIH arrhythmia database, IEEE Trans. Biomed. Eng. 33 (1986) 1157–1165.
- [11] MIT-BIH Database distribution, Massachusetts Institute of Technology, 77 Massachusetts Avenue, Cambridge, MA 02139, 1998.
- [12] American National Standard for Ambulatory Electrocardiographs, publication ANSI/AAMI EC38-1994, Association for the Advancement of Medical Instrumentation, 1994.
- [13] Q. Xue, Y.H. Hu, W.J. Tompkins, Neural-network-based adaptive matched filtering for QRS detection, IEEE Trans. Biomed. Eng. 39 (1992) 315–329.
- [14] C. Li, C. Zheng, C. Tai, Detection of ECG characteristic points using wavelet transforms, IEEE Trans. Biomed. Eng. 42 (1995) 21–28.
- [15] J. Lee, K. Jeong, J. Yoon, M. Lee, A simple real-time QRS detection algorithm, Proceedings of the 18th Annual International Conference of the IEEE Engineering in Medicine and Biology Society, Amsterdam, 1996.
- [16] A. Ruha, S. Sallinen, S. Nissila, A real-time microprocessor QRS detector system with a 1ms timing accuracy for the measurement of ambulatory HRV, IEEE Trans. Biomed. Eng. 44 (1997) 159–167.
- [17] J. Pan, W.J. Tompkins, A real time QRS detection algorithm, IEEE Trans. Biomed. Eng. 32 (1985) 230–236.
- [18] V.X. Afonso, W.J. Tompkins, T.Q. Nguyen, S. Luo, ECG beat detection using filter banks, IEEE Trans. Biomed. Eng. 46 (1999) 192–201.

**Diego S. Benitez** received an Engineering degree (CUM LAUDE) in Electronics and Control from the Escuela Politecnica Nacional, Quito, Ecuador in 1994, and a M.Sc. degree in Instrumentation and Analytical Sciences (Digital Instrumentation and Signal and Image Processing) from UMIST, Manchester, UK in 1997. He is presently completing his Ph.D. studies in Instrumentation and Digital Signal Processing (DSP) at UMIST. His professional interests are in DSP, intelligent sensor systems, biomedical instrumentation, industrial automation, digital systems and computing. Mr. Benitez is member of the IEEE and of the Institute of Physics.

**Patrick Gaydecki** is a Senior Lecturer in the Department of Instrumentation and Analytical Science at UMIST. He gained a 1st Class Honours Degree in Computing and Biology from the University of Demontfort in 1980, and his Ph.D. in Ecological Physics from the University of Cranfield in 1984. He is chartered physicist, a member of the Institute of Physics and the British Institute of Nondestructive Testing and is also currently Honorary Editor of the journal *Nondestructive Testing and Evaluation*. He has a keen interest in the development of real-time digital signal processing (DSP) hardware and software, based around modern high MIP-rate DSP devices. He has published over 60 papers relating to signal processing, having presented his work in Europe and the Americas.

**Amir Zaidi** received his medical degree from the University of Manchester, UK in 1989 and is a member of the Royal College of Physicians. He is currently working as a Specialist Registrar in Cardiology at the Manchester Heart Centre. His research interests include investigation and treatment of vasovagal syncope and the misdiagnosis of epilepsy.

**Adam P. Fitzpatrick** received his medical degree from St Bartholomew's Medical School, London, UK in 1982 and an M.D. from the University of London in 1990. Following a post-doctoral fellowship at The University of California, San Francisco he was appointed Consultant Cardiologist and Electrophysiologist at the Manchester Heart Centre. His principal interests are in mechanisms of vasovagal syncope and radiofrequency ablation. Dr. Fitzpatrick is a fellow of the Royal College of Physicians and the American College of Cardiology.